

Brief Reports

Brief Reports are short papers which report on completed research which, while meeting the usual Physical Review standards of scientific quality, does not warrant a regular article. (Addenda to papers previously published in the Physical Review by the same authors are included in Brief Reports.) A Brief Report may be no longer than $3\frac{1}{2}$ printed pages and must be accompanied by an abstract. The same publication schedule as for regular articles is followed, and page proofs are sent to authors.

Novel magnetoresistance oscillations in a two-dimensional superlattice potential

H. Fang and P. J. Stiles

Department of Physics, Brown University, Providence, Rhode Island 02912

(Received 23 October 1989; revised manuscript received 20 December 1989)

A new type of magnetoresistance oscillation in a two-dimensional electron gas modulated by a hexagonal lateral periodic electric potential has been observed in GaAs/Al_xGa_{1-x}As heterostructures. The magnetoresistance oscillations appear at very low magnetic field and the peak positions are directly determined by the magnetic field and the periodicity of the modulation structure. The experimental results can be understood by using a theoretical argument similar to those used in the one-dimensional case. Two kinds of results correlate with structures differing in degree of depletion and the resulting geometry.

As the lateral dimension of the two-dimensional electron gas is reduced and reaches the submicrometer range and becomes comparable with or smaller than the magnetic length $l = \sqrt{\hbar/eB}$, the standard Shubnikov-de Haas effect no longer exists because of the larger orbit size and a new type of magnetotransport phenomena is expected. Hofstadter¹ pointed out that the two-dimensional motion of electrons in a periodic potential and a perpendicular magnetic field generates a series of interesting commensurability effects. This problem can be studied experimentally in transport samples with a synthetic two-dimensional periodic submicrometer structure. Weiss *et al.*² first reported novel magnetoresistance oscillations in a two-dimensional electron gas modulated with a holographically induced one-dimensional periodic potential. They found that oscillation maxima arise whenever the classical cyclotron diameter $2R_c$ at the Fermi energy is a multiple of the period a , which can be explained as due to the oscillatory dependence of the bandwidth of the modulation-broadened Landau levels.³ Later, Winkler *et al.*⁴ published similar results obtained on electrostatically induced one-dimensional grid samples. In addition they observed a set of oscillations corresponding to a smaller spacing, $a/3$. The "one-third" set of oscillations is stronger than the integer one at positive gate voltages and the physical mechanism causing the "one-third" set has not been identified. Recently, some preliminary experimental results of magnetoresistance oscillations in a two-dimensional periodic potential with a square geometry have been reported.^{5,6} In this paper, we present observations of novel magnetoresistance oscillations with different oscillation frequencies and different phase factors observed in a hexagonal geometry two-dimensional superlattice potential.

The samples used in our experiments are conventional GaAs/Al_xGa_{1-x}As heterostructures grown by molecular-beam epitaxy with 1- μm GaAs buffer layer on top of a semi-insulating GaAs substrate, a 200- \AA undoped Al_xGa_{1-x}As spacer, a 500- \AA Si-doped Al_xGa_{1-x}As layer, and a 100- \AA GaAs cap layer. Typical samples with a Hall bar geometry have a sheet density in the range of $n_s = (2.4-4.3) \times 10^{11} \text{ cm}^{-2}$ and mobility of $\mu_n = (2.3-4.6) \times 10^5 \text{ cm}^2/\text{Vs}$ at $T = 4.2 \text{ K}$. With a new and simple technique utilizing a monolayer of close-packed uniform latex spheres as an etching mask in conjunction with reactive ion etching, periodic submicrometer structures with periodicity of 3300, 3640, and 3940 \AA have been formed by etching holes between the spheres.⁷ By adjusting the etching depth, two kinds of samples have been made for investigation by magnetoresistance measurements. The first kind of sample, the shallow-etched sample, is formed by just etching through the GaAs cap layer, stripping the balls, and then depositing the metal on the top of the structure. In this way, an electrostatic periodic electrical potential is generated. Schematic drawings of the periodic structure pattern and the shallow-etched sample profile are given in Figs. 1(a) and 1(b), respectively. The second kind of sample is the deep-etched sample where the etching holes go all the way through the two-dimensional electron gas layer to introduce a two-dimensional periodic carrier density distribution [see Fig. 1(c)]. The experiments are performed using standard lock-in amplifier techniques to measure the ac magnetoresistances at low modulation frequencies. In this paper, we will present the magnetoresistance data measured at transverse magnetic fields of 0–8 T and temperatures down to 1.3 K.

Figure 2 shows the experimental data of magnetoresis-

tance signal V_{xx} versus the magnetic field for two samples with 3300-Å periodic structure but different etching depths. Besides the normal Shubnikov-de Haas effect occurring at high magnetic fields, additional magnetoresistance oscillations are observed at the low magnetic field range (below 0.6 T). The oscillations are periodic in $1/B$ and have amplitudes that are smaller and the oscillatory frequency is slower than those in the Shubnikov-de

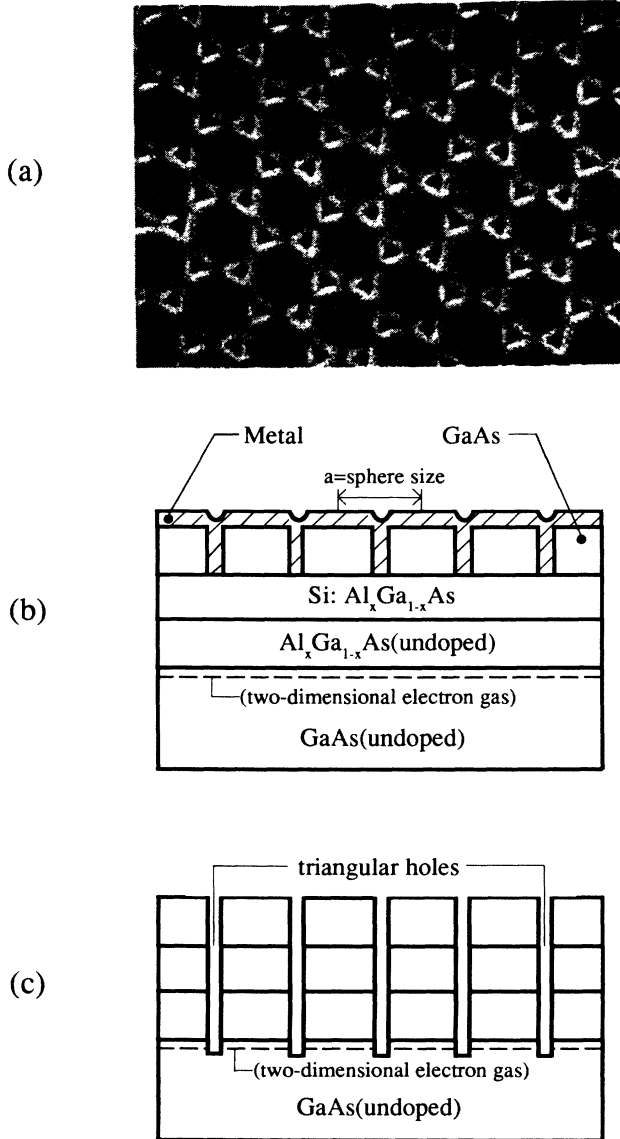


FIG. 1. The etching pattern and the schematic drawings of the periodic structure and sample profile: (a) a scanning electron microscope picture of the etched submicrometer structure of triangular hole array with a period of 3300 Å; (b) a cross-sectional view of the submicrometer periodic structure in the shallow-etched sample, with associated device information. The holes have been etched through the GaAs cap layer down to the surface of the Si:Al_xGa_{1-x}As layer. (c) The device profile for the deep-etched sample. Here the etching holes pass through the two-dimensional electron gas layer.

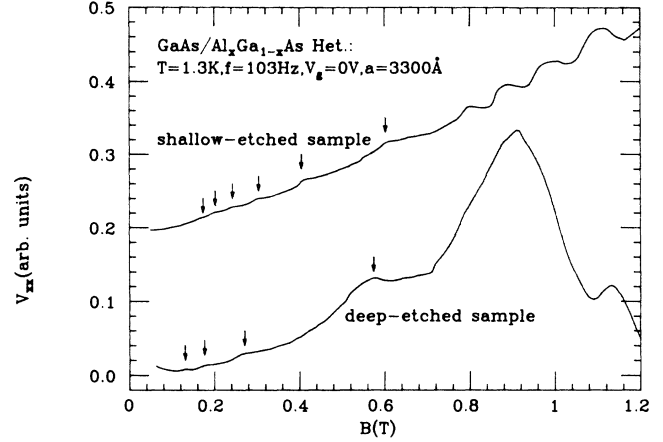


FIG. 2. The experimental data of the magnetoresistance vs the magnetic field for samples with modulation period of 3300 Å and different etching depths. The positions indicated by arrows are the magnetoresistance peaks due to the new oscillations.

Haas effect. A fan diagram of the integer number m versus $1/B$ for the two kinds of the samples (two deep-etched and two shallow-etched and gated samples) with different periodicities and gate biases is shown in Fig. 3. Basically, all the experimental points fit straight lines very well with a small error less than 2%. For the deep-etched samples, the peaks in the magnetoresistance occur at the magnetic field given by

$$2R_c = (m + \alpha)a, \quad m = 1, 2, 3, \dots, \quad (1)$$

where $R_c = 2\hbar k_f / eB$ is the classical cyclotron radius at the Fermi energy, $k_f = (2\pi n_s)^{1/2}$, and n_s is the average carrier density determined from the Shubnikov-de Haas oscillations. The value of the phase factor α from the measurements is about -0.21 ± 0.02 (which has the op-

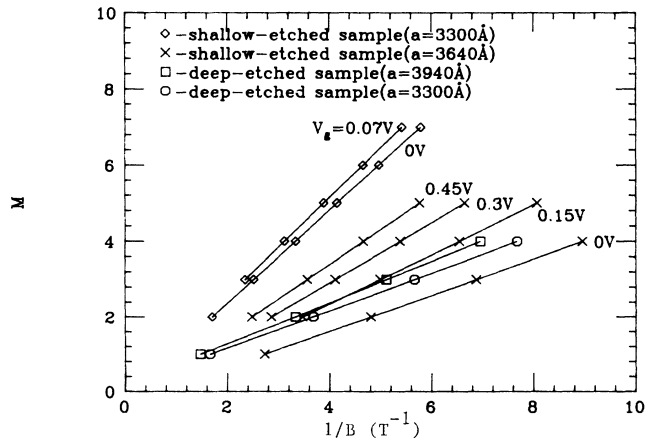


FIG. 3. The fan diagram of the integer number vs the reciprocal of the magnetic field for both kinds of samples with different periodicities and gate voltages. The experimental data are taken at $T = 1.3$ K and $f = 103$ Hz.

posite sign to that of Ref. 3). Also for the shallow-etched samples with different periodicities and gate voltages, the maxima appear at the following positions:

$$2R_c = (m + \beta)b, \quad m = 1, 2, 3, \dots, \quad (2)$$

with a phase factor $\beta = 0.27 \pm 0.04$ for the whole range of the gate biases and periodicities. The β value changes slightly with the gate voltage and becomes larger at lower gate voltages. In Eq. (2), b is equal to $a/2$, the half length of the period. It is noted that in magnetocapacitance measurements, no additional oscillations have been observed for the same devices. In order to clarify the experimental results, the unetched samples made from the same wafer have been checked. The unetched samples show no such additional magnetoresistance or capacitance oscillation structure.

For the deep-etching case, the etched holes pass through the two-dimensional electron layer. The carrier densities in those areas between the points of the triangles in Fig. 1(a) will have a lower density than the shallow-etched samples due to depletion effects. Upon considering the depletion effect, our system is an array of coupled quasiquantum dots with superlattice period equal to the size of the balls. Suppose that the modulation potential between the points is weak, then the potential variation with the positions of the spheres can be simply represented by a cosine function as shown in Fig. 4(a). Since the periodicity of this modulation potential is a , the oscillatory behavior in magnetoresistance [described by Eq. (1)] can be understood by its similarity to the one-dimensional case. In the shallow-etching case, the modulation potential is much weaker than in the previous one so that the circular two-dimensional electron regions fill all of two-dimensional space. The modulation potential at the triangular areas is higher than at the rest of the places and the electrons traveling along those regions affect the conductivity and modify the additional oscilla-

tions. Thus the geometry of the two-dimensional electron distribution changes from a hexagonal dot array for deep-etched samples to this special one given in Fig. 4(b) for shallow-etched samples because of the difference in degree of depletion. Comparing the modulation potential with the deep-etching one, the difference is that the distance between triangles in the shallow-etching case is smaller and roughly half the length of the spacing between the dots in the deep-etching case, if the amplitude size is ignored. Electrons in the shallow-etched samples pass through more potential barriers in a mean free path and that may cause the higher-frequency oscillation results given in Eq. (2).

Several semiclassical^{4,8} and quantum-mechanical^{3,9,10} calculations have been made for the one-dimensional periodic modulation potential,^{3,4,6-8} but no results have been published for a two-dimensional periodic modulation potential. With the assumption of a weak and cosinelike modulation potential, the two-dimensional modulation potential with a hexagonal geometry can be indicated as

$$V(x, y) = V_0 \left[\cos \left[\frac{2\pi x}{a} \right] + \cos \left[\frac{2\pi y}{\sqrt{3}a} \right] \right] \cos \left[\frac{2\pi y}{\sqrt{3}a} \right], \quad (3)$$

where the x axis is chosen in the same direction as in Fig. 4(a). Using the first-order perturbation method to calculate the matrix element $\langle n, x_0 | V(x, y) | n, x_0 \rangle$ with a chosen gauge $\mathbf{A} = (0, xB, 0)$ and an unperturbed harmonic oscillator wave function

$$\psi_{n, x_0}(x) = \frac{1}{L_y} e^{ik_y y} \phi_n(x - x_0)$$

centered at position $x_0 = -l^2 k_y$, an energy spectrum as in the case of a one-dimensional periodic potential³ can be derived, i.e., the modulation-broadened Landau bands oscillate with the magnetic field and the bandwidth at the Fermi energy vanishes when $2R_c = (m - 0.25)a$ and is maximal for $2R_c = (m + 0.25)a$ in the above two-dimensional periodic potential. One should recognize that there is a problem of using the above method for a two-dimensional periodic potential because the solution could be gauge dependent. This is due to a mistreatment of the degenerate perturbation problem with a nondegenerate wave function. The degeneracy in this case is extremely high and it makes the calculation for a two-dimensional periodic potential problem very difficult. Since the calculated results^{9,10} for one-dimensional modulation potential are consistent with the experimental data, we can use the results to interpret the experimental data for the two-dimensional periodic potential. In the one-dimensional case, the average velocities v_x and v_y are $\langle n, x_0 | v_x | n, x_0 \rangle = 0$ and

$$\langle n, x_0 | v_y | n, x_0 \rangle = -\frac{1}{m\omega_c} \frac{dE_n}{dx_0} \neq 0.$$

From the Kubo-type formula with the similar approximation,⁹ the average conductivity tensor is given as

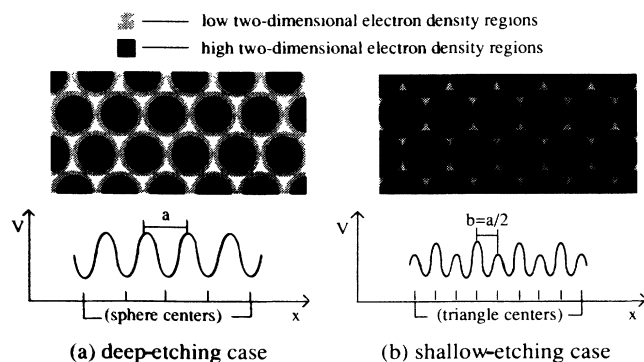


FIG. 4. The sketches of the carrier distributions and the modulation potentials for two kinds of devices: (a) an array of coupled quantum dots with a hexagonal geometry and the potential variation along one superlattice direction in deep-etched samples and (b) a triangle array with the special geometry and the resulting simplified modulation potential in shallow-etched samples.

$$\sigma_{\mu\mu}^- = -\frac{\hbar e^2}{l^2} \int dE \frac{df}{dE} \int_0^a dx_0 \frac{1}{a} \sum_{n,n'} |\langle n, x_0 | v_\mu | n', x_0 \rangle|^2 \times \text{Im} G_{nx_0}^- \text{Im} G_{n'x_0}^-, \quad (4)$$

where f is the Fermi distribution function and $G_{nx_0}^- = [E - E_n^{(1)}(x_0) - \Sigma^-(E)]^{-1}$ is the collision-broadened Green's function and the $\Sigma^-(E)$ is the quantum-number-independent self-energy. With the average velocity v_x equal to zero, the major contribution to the conductivity tensor σ_{xx} or ρ_{yy} comes from the density-of-states variation with the periodic potential. The density of states when the energy dispersion is zero, i.e., flat band, is maximal and it gives rise to maxima in σ_{xx} and ρ_{yy} . The nonzero average velocity v_y represents the contribution from the unperturbed Landau levels which dominates the oscillations of σ_{yy} or ρ_{xx} because there is no contribution due to the density-of-states variation in the y direction and this causes the measured resistivity ρ_{xx} to be a minimum at flat band. In the two-dimensional modulation case, we expect both component v_x and v_y to go to zero due to the modulation in all directions. Therefore the measured magnetoresistance ρ_{xx} shows maxima at flat bands. The oscillation signals from a two-dimensional modulation potential are much weaker because there are only a few electrons contributing to the off-diagonal matrix elements of the conductivity tensors. Hence the magnetoresistance oscillation in the deep-etched samples satisfies Eq. (1) with an opposite phase from the one-dimensional data. For the shallow-etched samples, the modulation potential is more complicated than the one in the deep-etched case. However, the basic

physical phenomena and oscillation mechanism are the same as the previous case. In shallow-etched samples, electron motion in some directions is free and in others is modulated by the periodic potentials. Therefore we expect the measured magnetoresistance oscillations to satisfy Eq. (2) with a positive phase factor as in the one-dimensional case. The experimental results for both kinds of samples with different periodicities are consistent with the quantum-mechanical ideas. With the above approach, the new oscillations in magnetoresistance result from the density-of-states oscillation with the magnetic field in a two-dimensional modulation potential, but the detailed physical mechanism for the higher-frequency oscillations is yet to be explained.

In conclusion, we have observed novel magnetoresistance oscillations in a two-dimensional electron gas modulated with a two-dimensional superlattice potential. This new type of oscillation comes from the fact that the Landau bandwidth as well as the density of states of a two-dimensional electron system modulated by a two-dimensional periodic potential oscillates with the magnetic field. The new oscillations only appear in the magnetoresistance measurements and the samples with etched periodic submicrometer structures. The differences of the oscillation period and phase factor in our experimental data between two kinds of samples correlate with different geometries due to the difference in degree of depletion.

We thank A. Houghton and A. Sudbo for the useful suggestions for the calculation, and T. P. Smith III and S. L. Wright for providing us heterostructure materials. This work is supported in part by the National Science Foundation Grant No. DMR-87-17817.

¹D. Hofstadter, Phys. Rev. B **14**, 2239 (1976).

²D. Weiss, K. v. Klitzing, K. Ploog, and G. Weimann, in *High Magnetic Fields in Semiconductor Physics II*, Vol. 87 of *Springer Series in Solid-State Science*, edited by G. Landwehr (Springer, Berlin, 1988), p. 357.

³R. R. Gerhardts, D. Weiss, and K. v. Klitzing, Phys. Rev. Lett. **62**, 1173 (1989).

⁴R. W. Winkler, J. P. Kotthaus, and K. Ploog, Phys. Rev. Lett. **62**, 1177 (1989).

⁵D. Weiss, K. v. Klitzing, K. Ploog, and G. Weimann, Surf. Sci.

(to be published).

⁶P. H. Beton, E. S. Alves, M. Henini, L. Eaves, P. C. Main, O. H. Hughes, G. A. Toombs, S. P. Beaumont, and C. D. W. Wilkinson, J. Phys. Condens. Matter (to be published).

⁷H. Fang, R. Zeller, and P. J. Stiles, Appl. Phys. Lett. **55**, 1433 (1989).

⁸C. W. J. Beenakker, Phys. Rev. Lett. **62**, 2020 (1989).

⁹R. R. Gerhardts and C. Zhang, Surf. Sci. (to be published).

¹⁰P. Vasilopoulos and F. M. Peeters, Phys. Rev. Lett. **63**, 2120 (1989).

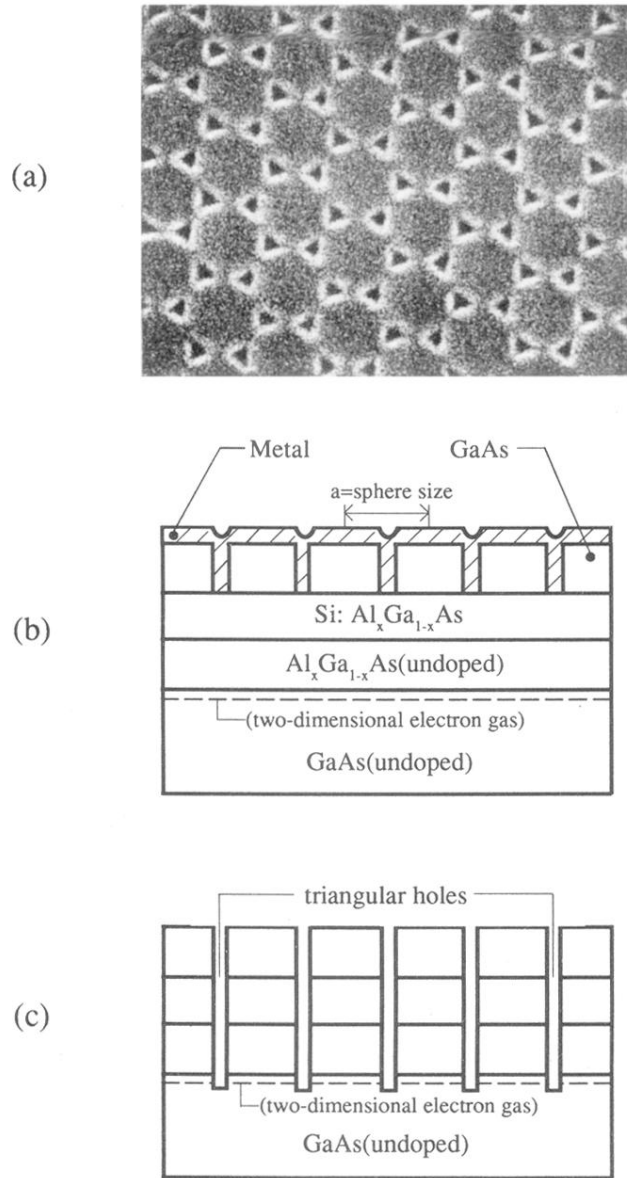


FIG. 1. The etching pattern and the schematic drawings of the periodic structure and sample profile: (a) a scanning electron microscope picture of the etched submicrometer structure of triangular hole array with a period of 3300 \AA ; (b) a cross-sectional view of the submicrometer periodic structure in the shallow-etched sample, with associated device information. The holes have been etched through the GaAs cap layer down to the surface of the $\text{Si:Al}_x\text{Ga}_{1-x}\text{As}$ layer. (c) The device profile for the deep-etched sample. Here the etching holes pass through the two-dimensional electron gas layer.

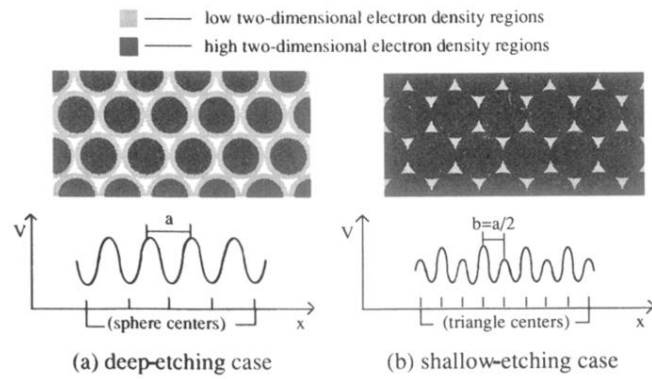


FIG. 4. The sketches of the carrier distributions and the modulation potentials for two kinds of devices: (a) an array of coupled quantum dots with a hexagonal geometry and the potential variation along one superlattice direction in deep-etched samples and (b) a triangle array with the special geometry and the resulting simplified modulation potential in shallow-etched samples.